Print ISSN 1110-208X

Online ISSN 2357-0016

Original article

Histological Study on the Effect of Taurine on Cisplatin Induced Sciatic Nerve Neuropathy in Adult Male Albino Rats

Shereen M. Mostafa , Maysara A. Salem, Hamdy A. Mohamed, Enas Elgendy

Department of Histology and Cell Biology, Faculty of Medicine; Benha University. Egypt.

Correspondence to: Shereen M. Mostafa, Department of Histology and Cell Biology, Faculty of Medicine; Benha University. Egypt.

Email:
sherinehassan548@gmail.com

Received:
Accepted

Abstract

Background: Cisplatin (CIS) is a powerful anti-neoplastic medication, it has adverse effects including peripheral neuropathy. Taurine (Tau) protects the cells by stabilizing membranes, regulating calcium levels, antioxidant and modulating apoptosis and inflammation. Objective: evaluate the protective impact of Tau on peripheral neuropathy caused by CIS. Materials and Methods: 45 healthy adult male albino rats spanning 150 to 250 grams were indiscriminately assigned to four groups. Group I: control group. Group II (CIS group): animals were administered intraperitoneal (IP) injection of CIS at a dosage of 2.5 mg/kg/day, with treatments biweekly throughout four-weeks duration Group III (CIS+Tau): Four days prior to the CIS injection, Tau was administered orally by gavage (250 mg/kg/day), Tau then continued for four weeks. Group IV (Tau group): Tau given orally (250 mg/ kg/ day) daily for four weeks. Sciatic nerve samples were obtained and prepared for light and electron microscopy evaluation. Results: Group II showed disorganized nerve bundle architecture and wide separation of nerve fibers. Nuclei of Schwann cells (SC) were small and darkly stained (pyknotic). Inflammatory cell infiltrate was observed. A statically significant difference in collagen fiber deposition (P <0.01) was observed relative to group I. Sciatic nerve by electron microscopy exhibited degenerative changes affecting myelin sheaths and axons. Group III exhibited partial improvement in certain histological features and a decrease in collagen fibres content that was statistically significant (P < 0.01) in comparison to Group II. Conclusion: This work concluded that Tau can mitigate CIS- induced peripheral neuropathy.

Key Words: CIS, Sciatic nerve, Peripheral neuropathy, Tau.

Introduction

Cisplatin is used for treatment of a broad spectrum of solid pediatric and adult malignancies tumors, like bladder, lung, testis, ovarian, head and neck cancers, cervical carcinoma and osteosarcoma and lymphomas [1].

The major toxicities that arise from CIS therapy is nephrotoxicity which is the biggest challenge associated with CIS treatment. Neurotoxicity, hematological toxicity, ototoxicity and gastrointestinal toxicity are also common. retinal toxicity, hepatotoxicity, cardiotoxicity, allergy and reproductive side effects have been reported. In addition, secondary malignancies may occur [2].

Sciatic nerve is the largest and thickest nerve in humans, emerging from the greater sciatic foramen of pelvis typically inferior to the piriformis muscle and descending along the posterior aspect of the thigh toward the knee [3].

Peripheral neuropathy is a prevalent neurological problem in the general population. It has common etiologies as diabetes mellitus, alcoholism, renal insufficiency and neurotoxic substances (e.g., chemotherapies, medications). The rare causes of peripheral neuropathy include neoplastic, viral, immune-mediated and hereditary causes [4].

When peripheral neuropathy arises as a consequence of chemotherapy, it is termed chemotherapy-induced peripheral neuropathy (CIPN). It is a prevalent iatrogenic complication associated with numerous antineoplastic medications, most frequently manifesting with sensory symptoms more so than motor deficits in a symmetrical distribution affecting hands and feet 'glove and stocking'. Sensory manifestations include thermal sensitivity tingling and numbness, while motor manifestations may involve muscle weakness leading to impaired balance or reduced dexterity. Symptoms of CIPN are frequently typically mild at onset but may progressively worsen with continued chemotherapy, potentially leading to significant impairments in long-term function, increased fall risk, and diminished quality of life [5].

Taurine, a sulfur-containing β-amino acid (2-aminoethanesulfonic acid), is mainly present in skeletal muscles, heart and brain. Also, it is found in various dietary sources, including dairy products, fish and meat [6].

Taurine is predominantly located in the intracellular compartment of various tissues, one of its key functions is maintaining osmotic balance and ensuring cell integrity. Tau conjugates with bile acids in liver yielding bile salts, that promote the emulsification, breakdown, and absorption of dietary fats in the intestines. This process is essential for efficient metabolism of lipid and absorption of fat-soluble vitamins (A, D, E, and K) [7]. Tau modulates calcium signaling and neurotransmission. It exerts antioxidant effects that likely contribute to its observed physiological benefits [8].

Material and Methods

Type of study: An experimental study.

Drugs and Chemicals

Cisplatin:

Cisplatin was made by Mylan, France, and was purchased from Pfizer chemical company (USA**)** in the form of vials at a concentration of 50 mg/ 50 mL. CIS (2.5 mg/kg/day) was injected IP, twice per week for a duration of four weeks [9].

Taurine:

Taurine, manufactured by Alpha Chemika (Mumbai, India) and obtained from Sigma (St. Louis, MO,

USA), was supplied in powder form and dissolved in distilled water(DW). It is used in doses (250 mg /kg/day) orally daily given four days before the injection of CIS and then continued administration daily for four weeks [10].

Animals and Diet:

Forty-five healthy adult male albino rats whose weights ranged from 150 to 250 grams of weight range, were acquired and maintained at animal facility of the Faculty of Veterinary Medicine, Moshtohor, Benha University. Rats were kept in standard cages under strict hygienic conditions and regular care and received water and balanced diet regularly. Animal handling procedures were conducted in compliance with established ethical guidelines. The experimental design was validated by the Ethical Committee of Benha University, Benha, Egypt (Approval code: MS.10.5.2023).

Experimental Study Design:

An experimental study was performed in January 2024 for four weeks. After a week of acclimatization, rats were assigned to four groups in a randomized fashion:

- **Group I (Control group; n=15):** It was further partitioned into three equal subgroups. Subgroup IA: underwent no experimental manipulation. Subgroup IB: I.P administration of 0.5 mL normal saline (CIS vehicle), was performed twice weekly over a four-week period. Subgroup IC: Rats were gavaged daily with 1 mL DW (the vehicle for Tau).
- **Group II (CIS group; n=10):** CIS (2.5 mg/kg/d) administered IP twice weekly over a period of four weeks [9]. The infusion concentrate, provided in 50 mL vials containing 1 mg/mL CIS, was dosed at 0.5 mL per rat,
- **Group III (CIS + Tau group; n=10):** Rats were treated with Tau at a dose of 250 mg/kg/day, administered orally by gavage [10]. Tau treatment commenced four days prior to the first CIS injection and continued daily for the entire four-week experimental period. In this study, each rat weighed approximately 200 gm and was administered 50 mg of Tau dissolved in 1ml DW. In addition, CIS was administered as described in Group II
- **Group IV (Tau group; n=10):** Rats received Tau (250 mg/kg /day) dissolved in DW via mouth gavage, each rat received 1ml of Tau hydrate daily for four weeks.

Sampling:

Four weeks after the initiation of the study, the rats underwent anesthesia via diethyl ether vapor inhalation and euthanized by cervical dislocation. The sciatic nerve was then excised, fixed in 10% NBF (neutral-buffered formaldehyde solution) and prepared for further histological analysis under light microscopy. For electron microscopic preparation, samples were initially fixed in 2.5% glutaraldehyde, then post-fixed in 1% osmium tetroxide to preserve ultrastructural integrity.

Histological Studies

Sections of paraffin-embedded tissue (5–7 µm) were stained with hematoxylin and eosin (H&E) to examine histopathological alterations across the experimental groups. Moreover, Sections were subjected to Masson's trichrome stain to analyze collagen fiber deposition [11].

Transmission Electron Microscopic (TEM) study [12]

Semi-thin sections were treated with Toluidine blue. Later, ultrathin sections (80 nm thick) were obtained from certain areas using glass knife. All steps were carried according to standard protocol [12]. Grids were scanned and images were captured by

JEOL JEM-1400 Plus transmission electron microscope (JEOL Ltd., Akishima, Tokyo, Japan) at the Electron Microscopy Unit, Faculty of Science, Alexandria University, El Shatby.

Morphometric Study and Statistical Analysis

Collagen deposition was quantified as the mean percentage area utilizing Image-Pro Plus software version 6.0 (Media Cybernetics Inc., Bethesda, Maryland, USA), based on the analysis of ten images from seven distinct, non-overlapping fields per group. All collected measurements were aggregated and subjected to statistical evaluation by IBM SPSS Statistics (Version 22; IBM Corp., Armonk, NY, USA). Intergroup differences were analyzed via one-way analysis of variance (ANOVA), with subsequent pairwise comparisons using the Least Significant Difference (LSD) post hoc test. Data are presented as mean (M) ± standard deviation (SD), a p-value < 0.01 indicated statistical significance.

Results

H & E Stain results (Fig. 1A- H):

- **Group I (Control group):**
  All subgroups of this group showed normal histological structure of the sciatic nerve. Nerve bundles were enclosed by a perineurial sheath, while individual nerve fibers were embedded within a loose connective tissue of the endoneurium. Nerve fibers appeared densely packed and parallel, with thick myelin sheaths that appeared dissolved or washed out due to their lipid content. The nuclei of SCs were observed to be regular in shape (**Fig. 1**A& B).
- **Group II (CIS group):**
  This group showed disorganized nerve bundle architecture. Nerve fibers were widely separated from each other due to the loss of some nerve fibers which showed multiple vacuolations, and degenerated and fragmented axons. SCs nuclei appeared reduced in number, with some exhibiting small, darkly stained pyknotic nuclei. Additionally, blood vessels appeared congested, accompanied by noticeable infiltration of inflammatory cells. (**Fig.1**C& D).
- **Group III (CIS + Tau group):**
  Sciatic nerve sections from group III exhibited nerve fibers that were largely similar to their normal histological appearance. The nerve bundles were well-encapsulated by perineurial sheath. Well organized nerve fibers, with most showing normal axons, thick dissolved myelin sheath while others showed some vacuolations. Some separation and a few inflammatory cells were still present **(Fig. 1E&** F).
- **Group IV (Tau group):**
  Sciatic nerve sections of group IV displayed normal histological structure, individual nerve fibers were embedded in the loose connective tissue of the endoneurium. Nerve fibers seemed acidophilic, parallel, and well packed with SCs nuclei between them. Nodes of Ranvier appeared as a constriction of the neurilemmal sheath. The nerve bundles were encapsulated by the perineurium (**Fig.1**G& H).

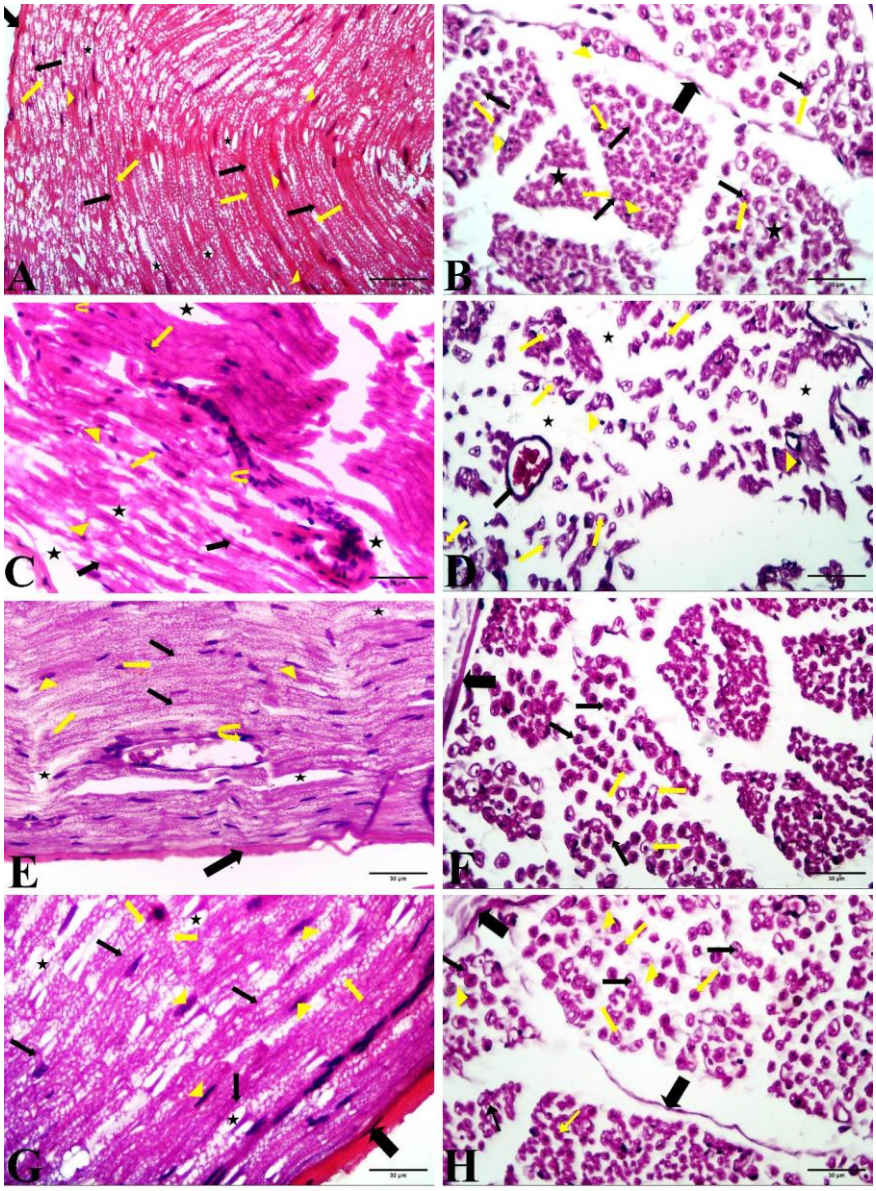

Fig. 1A-H: (A) Group I; a longitudinal section (L.S) of the sciatic nerve demonstrates a portion of nerve bundle surrounded by perineurium (thick arrow) with closely arranged, packed, and parallel nerve fibers revealing axons (thin black arrows) with thick dissolved myelin sheath (thin yellow arrows). Schwann cells nuclei is observed between the nerve fibers (arrowheads). Nodes of Raniever (stars), **(B) Group I;** a transverse section (T.S) of sciatic nerve showing nerve bundles enclosed by perineurium (thick arrow) with closely arranged myelinated nerve fibers revealing acidophilic axons (thin black arrows), enclosed by clear areas representing washed out myelin sheaths (yellow arrows). Schwann cells nuclei are apparent (arrowheads). Endoneurium (stars) surrounds each nerve fiber**, (C) Group II (CIS group);** a L.S of the sciatic nerve displaying poorly organized nerve bundle architecture. Separation of nerve fibers (stars). Nerve fibers appear degenerated and corrugated (thick arrows). Thin yellow arrows refer to nuclei of Schwann cells which are apparently decreased, small darkly stained pyknotic nucleus (arrowheads) and inflammatory cell infiltrate (curved arrows). **(D) Group II (CIS group);** a T.S of the sciatic nerve showing disorganized nerve bundles architecture which are widely separated from each other. Degenerated nerve fibers reveal multiple vacuolations (thin yellow arrows) and wide separation between nerve fibers (stars). Schwann cells nuclei appear shrunken and darkly stained (arrowheads). A blood vessel appears dilated and congested (thin black arrow), **(E) Group III (CIS+Tau)**; a L.S of sciatic nerve shows nerve fibers that are largely similar to their normal histological structure. The nerve bundle is enclosed by perineurium (thick arrow). Nerve fibers appear well arranged revealing axons (thin black arrows) and dissolved myelin sheath (thin yellow arrows) Schwann cell nuclei (arrowheads). The separation between nerve fibers (stars) and some mononuclear inflammatory cell infiltration is still present (curved yellow arrow)**, (F) Group III**

(CIS+Tau); a T.S of sciatic nerve exhibiting nerve fibers are closely arranged and largely similar to their normal histological structure. The nerve bundle is surrounded by perineurium (thick arrow). The majority of the nerve fibers reveal normal axons (thin black arrows) while others show some vacuolations (thin yellow arrows)**, (G) Group IV (Tau group);** a L.S of sciatic nerve revealing well organized nerve fibers similar to normal histological structure. Part of the nerve bundle is surrounded by perineurium (thick arrow) with closely arranged, packed, and parallel nerve fibers revealing axons (thin black arrows) with thick dissolved myelin sheath (thin yellow arrows). Schwann cells nuclei(arrowheads) are well observed among the nerve fibers. Nodes of Ranvier (stars) can be seen**, (H) Group IV (Tau group);** a T.S of sciatic nerve displaying well-organized nerve fibers greatly similar to normal histological structure. The nerve bundle is enclosed by perineurium (thick arrow) and closely arranged myelinated nerve fibers revealing acidophilic axons (thin black arrows), enclosed by a clear area representing dissolved myelin (thin yellow arrows). Schwann Cells nuclei are apparent (arrowheads). **(H&E X400)**

Masson trichrome staining results (Fig. 2A-D):

- **Group I (control group):** exhibited limited accumulation of collagen among the nerve fibers (**Fig.2**A).
- **Group II (CIS group):** demonstrated substantial collagen fiber deposition among the nerve fibers (**Fig. 2**B).
- **Group III (CIS + Tau group):** revealed less pronounced collagen fibers accumulation among the nerve fibers (**Fig. 2**C).
- **Group IV (Tau group):** demonstrated slight collagen accumulation among the nerve fibers (**Fig.** 2D).

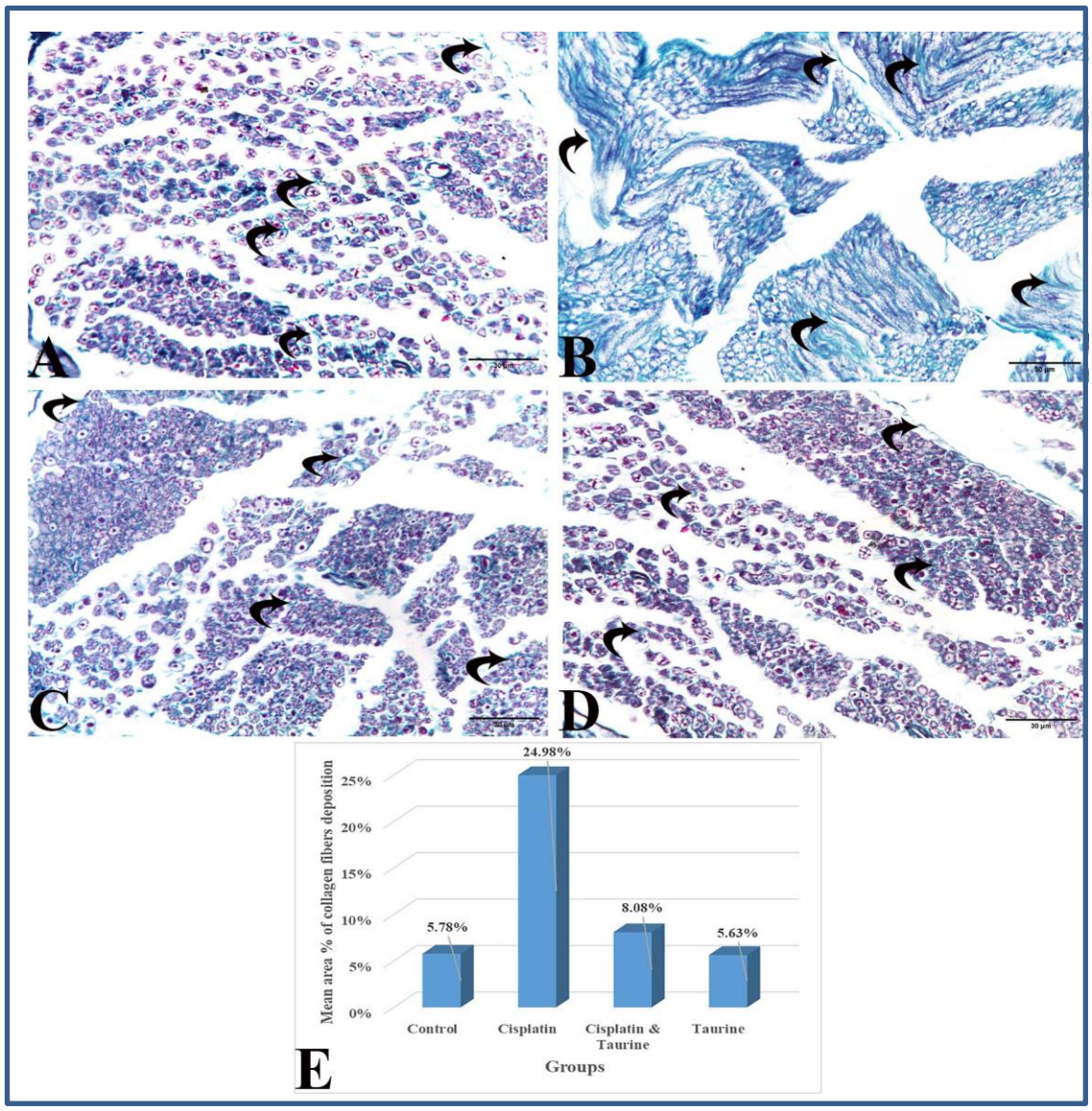

Fig. 2A-D: (A) A transverse section (T.S) of sciatic nerve from group I reveals limited collagen fibers among the nerve fibers (curved arrows), **(B) Group II (CIS group);** displays pronounced collagen deposition among the nerve fibers (curved arrows), **(C) Group III (CIS+Tau group);** exhibits mild collagen deposition among the nerve fibers (curved arrows), **(D) Group IV (Tau group);** reveals minimal collagen deposition among the nerve fibers (curved arrows), **(E) A histogram;** displaying the mean percentage area of collagen accumulation in experimental groups. **(Masson trichrome staining X400).**

Morphometric and Statistical Results

The histogram in Figure 2E illustrates the mean percentage area ± SD of collagen fiber content for all groups. Collagen fibers deposition significantly reduced ($P < 0.01$) in group III relative to group II. While, it increased significantly ($P < 0.01$) in group III relative to group I. There was an insignificant difference ($P > 0.01$) of collagen content in group IV in comparison with group I.

Table (1): Showing the mean area % and SD of collagen fibers deposition for all groups with comparison between groups by Post Hoc LSD test.

	Group I	Group II	Group III	Group IV
Mean area %	**5.78 %**	**24.98 %**	**8.08 %**	**5.63 %**
SD	**0.3366**	**0.2825**	**0.2602**	**0.3255**
Significance (sig.) at P < 0.01	**2,3**	**1,3,4**	**1,2,4**	**2,3**

1=sig. with group I 2=sig. with group II 3=sig. with group III 4=sig. with group IV

Toluidine blue staining results (Fig. 3A-D):

Group I (control group): sciatic nerve showed normal histological structure. The nerve bundle appeared with closely arranged and variable-sized nerve fibers. Perineurium surrounded the nerve bundles. Minimal endoneurial connective tissue was observed between the nerve fibers. Dark blue rings representing myelin sheaths were seen surrounding lightly stained blue axons, scattered groups of thinly myelinated nerve fibers were also present, and SCs appeared around some nerve fibers (**Fig. 3**A).

Group II (CIS group): The sciatic nerve section of group II exhibited variable histological changes in the myelin sheath as vacuolations and thinning of myelin sheath. Some nerve fibers showed splitting and degenerated myelin and separation of axons from myelin sheaths. Some axons showed shrinkage and atrophy and a few fibers showed degenerated axons (**Fig. 3**B).

Group III (CIS+Tau group): The myelin sheaths within the sciatic nerve bundles appeared dense and well-organized, nearly similar to that of group I. Nevertheless, a few fibers exhibited vacuolations and splitting of the myelin (**Fig.3**C).

Group IV (Tau group): The sciatic nerve bundle showed normal histological structure of nerve fibers. The nerve bundle was enclosed by the perineurium and contained cross sections of myelinated nerve fibers of variable sizes. Dark blue rings of intact myelin surrounded clear axons and scanty endoneurial connective tissue around each nerve fiber. SCs appeared around some nerve fibers (**Fig. 3**D).

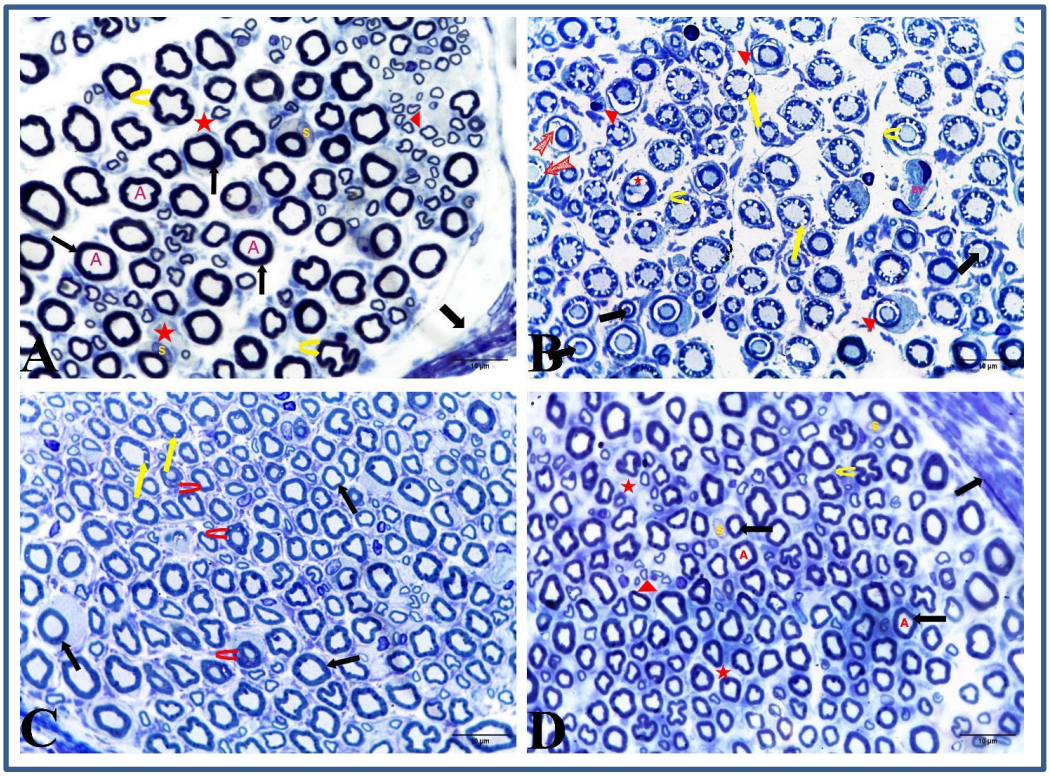

Fig.3A-D: (A) A semithin section of sciatic nerve from group I exhibiting part of the nerve bundle with multiple closely arranged myelinated nerve fibers. Intact myelin sheath is visible as deeply stained blue circles (thin arrow) encircling lightly stained axons. (A) Endoneurium (stars) surrounds each nerve fiber and perineurium (thick arrow) surrounds the nerve bundle. The majority of the myelinated nerve fibers are ensheathed by schwann cells (s). Thin myelinated nerve fibers (arrowhead) are noticed. Axon fluting (curved arrows) which appears as infolding of myelin sheath in proximity to nodes of Ranvier, **(B) Group II (CIS group);** showing degenerated nerve fibers. Myelinated nerve fibers show multiple vacuolations (yellow arrows), thinning of myelin (arrowheads), degenerated and fragmented myelin (bifid arrows), Some axons show shrinkage (black arrows) and splitting from myelin sheath (curved arrows). Blood vessel is present (BV). Few fibers show degenerated axon (star), **(C) Group III (CIS+Tau group);** restored structural integrity of the sciatic nerve is noticed. Most fibers are normal (thin black arrows), apart from some fibers with vacuolated myelin sheaths (thin arrows). Few fibers show degenerated and fragmented myelin sheath (curved red arrows), **(D) Group IV (Tau group)**; shows normal histological structure. Normal axons with normal myelin sheath. Endoneurium surrounding each nerve fiber (star) and perineurium surrounding each nerve bundle (thick arrow). Regular myelin sheaths (thin black arrows) surrounding lightly stained axons (A) Schwann cell surrounds most myelinated nerve fibers (S). Thin myelinated nerve fibers (arrowhead) are noticeable. Axon fluting (curved arrow) is also seen. **(Toluidine blue X1000)**

Electron Microscopy results (Fig. 4A-H):

Group I (control group): demonstrated normal myelinated and some unmyelinated nerve fibers. Myelin sheaths were observed as dense compact lamellae enclosing the axoplasm. SCs wrapped around the axons forming a multilayer of myelin sheaths. The axoplasm exhibited normal ultrastructure, containing neurofilaments, microtubules, and morphologically intact mitochondria. Collagen fibers were observed within the endoneurium. The unmyelinated nerve fibers were observed in clusters (**Fig. 4** A, B).

Group II (CIS group): exhibited degenerative changes affecting myelin sheaths and axons. There was splitting of the myelin sheath (the well packed lamellar structure of myelin sheath was lost) Also, SCs surrounding myelinated nerve fibers showed a small nucleus with an irregular outline, increased perinuclear space, and slightly dilated

rough endoplasmic reticulum. Bundles of collagen fibers were observed in the endoneurium (**Fig.4** C, D).

Group III (CIS+Tau group): most myelinated nerve fibers revealed well-compacted myelin sheath with stippled appearance of the axoplasm due to neurofilament. SCs showed normal nuclei, rough endoplasmic reticulum, and mitochondria but still, some fibers showed degenerative changes with the splitting of the myelin sheath (**Fig. 4** E, F).

Group IV (Tau group): demonstrated regular compact myelin sheaths. Microtubules and neurofilaments were seen in the axoplasm. SC cytoplasm formed a coat around the myelinated nerve fibers (**Fig.4** G, H**)**.

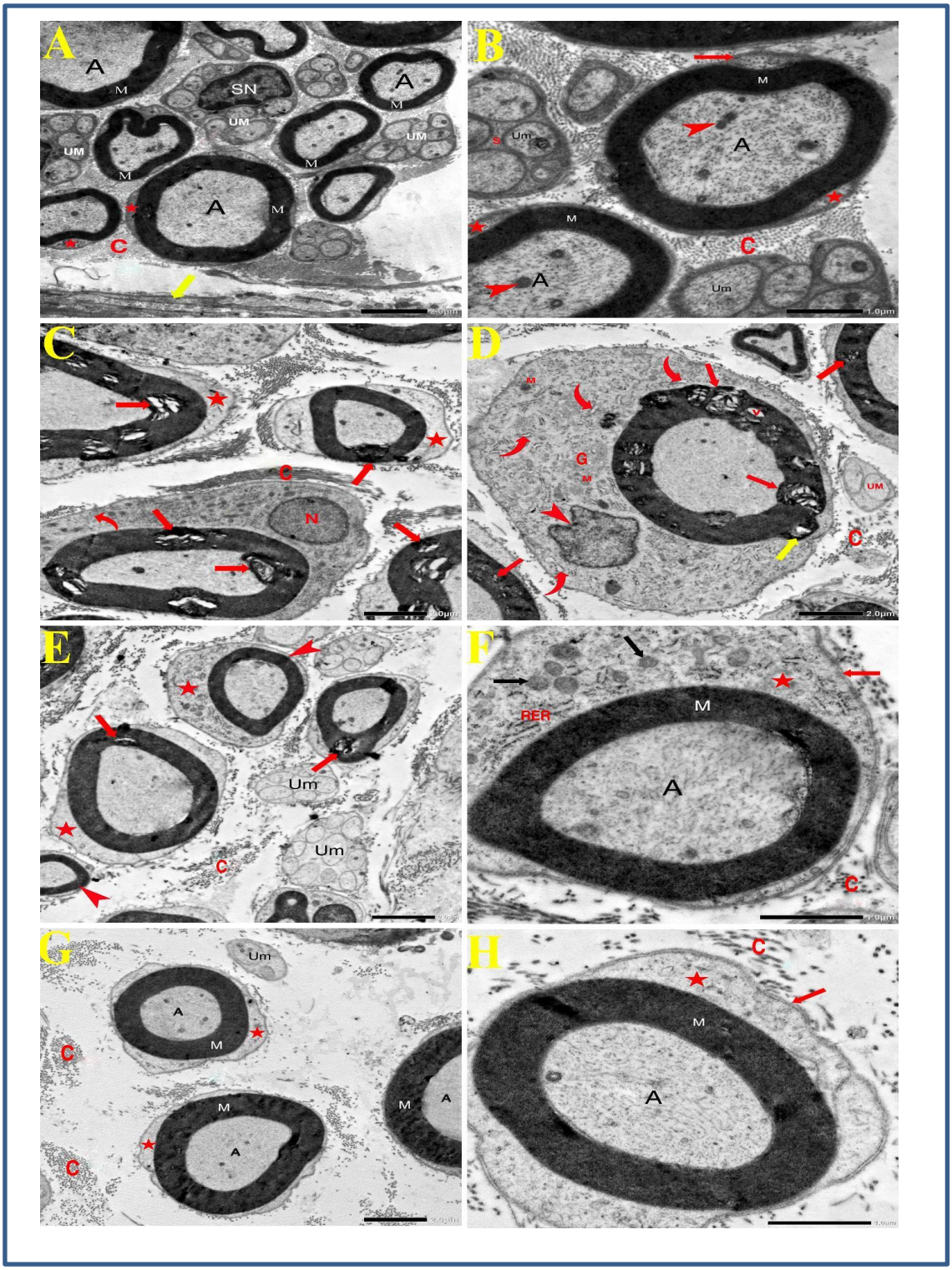

Fig. 4A-H: (A) A transmission electron micrograph (TEM) of sciatic nerve of group I displaying nerve fibers surrounded with well compacted myelin sheath (M) with a stippled appearance of axoplasm (A). Schwann cell nucleus (SN) enveloping bundle of unmyelinated axons (um). Schwann cell cytoplasm is noticed forming a rim around myelinated nerve fibers (stars). Among the nerve fibers endoneurium is seen containing collagen fibers (C). Perineurium surrounds a bundle of nerve fibers (yellow arrow) **(TEM X2500)** (**B) Group I;** showing myelinated nerve fibers which reveal well-compacted myelin sheath (M) with the stippled appearance of axoplasm (A) due to neurofilaments. Normal mitochondria (arrowheads) is noticed. Schwann cell forms a coat around myelinated nerve fibers (Stars). The red arrow refers to the basal lamina of the Schwann cell. Schwann cell (S) enveloping a bundle of unmyelinated axons of variable size (Um). Among the nerve fibers endoneurium is noticed containing collagen fibers (C) **(TEM X8000) (C) Group II (CIS group);** exhibiting degenerated myelinated nerve fibers which reveal focal areas of splitting within myelin sheath and wide separation of myelin lamellae (red arrows). Schwann cell forms a coat around myelinated nerve fiber (stars). Schwann cell nucleus (N) and Schwann cell cytoplasm (curved arrow) are noticed. Collagen fibers are seen in endoneurium (C) **(TEM X2500), (D) Group II (CIS group);** showing degenerated myelinated nerve fiber with focal areas of splitting within myelin sheath (red arrows), vacuolation (v) and evagination of the myelin sheath (yellow arrow) surrounded by Schwann cell which appears with small indented nucleus and irregular outline (arrowhead). Schwann cell cytoplasm shows rough endoplasmic reticulum, some show slight dilation (curved arrows), normal mitochondria (M), and Golgi apparatus (G). Collagen fibers are seen in endoneurium (C). Unmyelinated fibers (UM) are noticed **(TEM X8000), (E) Group III (CIS+Tau);** showing some myelinated nerve fibers which retain compact regular myelin sheath lamellae (arrowheads) with some fibers reveal few areas of minimal focal splitting of myelin sheath lamellae (arrows). The cytoplasm of schwann cell is enveloping the myelin sheath (stars), A group of unmyelinated fibers is noticed (Um). Collagen fibers are seen in endoneurium (C) **(TEM X2500), (F) Group III (CIS+Tau);** showing myelinated nerve fiber which retains well compacted dense myelin sheath appearance (M) with normal stippled appearance of the axoplasm due to presence of neurofilaments (A), Schwann cell is seen forming a coat around myelin sheath (star) with normal mitochondria (black arrows) and rough endoplasmic reticulum (RER), External lamina of Schwann cell is noticed (red arrow). Collagen fibers are seen in endoneurium (C) **(TEM X8000), (G) Group IV (Tau group)**; showing normal nerve fibers with well compacted regular myelin sheath (M) with homogenous axoplasm (A). Schwann cell forms a coat around myelinated nerve fibers (Stars). Unmyelinated axons of variable size (Um) are noticed. Collagen fibers of endoneurium (um) are seen. **(TEM X2500), (H) Group IV (Tau group)**; showing a myelinated nerve fiber which reveals regular myelin sheath (M) with a stippled appearance of axoplasm (A). Schwann cell cytoplasm forms a coat around the myelinated nerve fibers (star). External lamina of Schwann cell (red arrow) is seen. Collagen fibers are seen in endoneurium (C) **(TEM X8000)**.

Discussion

This study was conducted using adult male albino rats to assess the potential neuroprotective impacts of Tau in CIS-induced peripheral neuropathy.

Chemotherapeutics are routinely utilized for the treatment of varying types of malignancies. CIPN is recognized as the most prevalent neurological complication caused by chemotherapeutics. It is a distressing side effect that can greatly reduce the quality of life in affected patients [13].

Cisplatin exhibits a molecular affinity for peripheral nerves, which are particularly vulnerable due to the absence of vascular and lymphatic barriers. This structural characteristic increases their susceptibility to the accumulation of cisplatin residues. Additionally, nerves are particularly vulnerable to oxidative stress, primarily as a result of their rich phospholipid composition and the axoplasm that is rich in mitochondria. Furthermore, they possess relatively weak cellular antioxidant defense mechanisms. [14]

Injury to peripheral nerves impairs the function of sensory, motor, and autonomic fibers. Unlike central nerves, peripheral nerves possess a degree of intrinsic regenerative ability. This regenerative capacity is primarily attributed to SCs, specialized neuroglial cells that are exclusive to the peripheral nervous system (PNS). Consequently, understanding the physiological alterations and functional roles of SCs during nerve repair may provide valuable insights for developing innovative therapeutic strategies [15].

Cancer survivors are significantly affected by CIPN. Currently, there is no universally accepted benchmark for the management of CIPN. Therefore, elucidating the fundamental mechanisms prompting CIPN is essential for developing more effective treatment strategies [16].

Taurine, is an amino acid present in nerves and muscles. It is abundant in meat and seafood. Tau is vital for maintaining cell membranes integrity. It exhibits anti-inflammatory properties, modulates intracellular calcium levels crucial for cell signaling, and maintains the balance of neurotransmitters to support proper neural function [17].

Herein, H&E staining of sciatic nerve of CIS group exhibited disrupted nerve bundle architecture, with several nerve fibers dissociated from the surrounding perineurium. Nerve fibers appeared widely spaced, likely due to axonal loss, and showed multiple vacuolations, degeneration, and fragmentation. A reduction in SCs nuclei was noted, many of which were small, darkly stained, and pyknotic. Additionally, blood vessels appeared congested, and focal inflammatory infiltrate was observed. These observations are in agreement with previous studies [18-22].

Peripheral neuropathy is closely linked to oxidative stress. Peripheral nerves are vulnerable to oxidative damage that triggers lipid peroxidation, inflammatory responses, and degradation of the myelin because of relatively poor cellular antioxidant activities [19, 21, 23-25].

Cisplatin leads to a decrease in key antioxidant enzymes like glutathione peroxidase (GPx) and superoxide dismutase (SOD), accompanied by an elevation in the oxidative marker malondialdehyde (MDA). This redox disequilibrium, characterized by a predominance of oxidants over antioxidants, is defined as 'oxidative stress'. CIS-induced oxidative stress damages the nervous tissue, causing demyelination and axonal degeneration. Depletion of antioxidants due to increased ROS and nitric oxide (NO) exacerbates injury, particularly in long axons with high phospholipid content and the axoplasm is rich in mitochondria. Studies have demonstrated that axonal cytotoxicity contributes to CIPN [14, 26].

Fumagalli et al. (2021) [27] reported that CIS caused axonal degeneration and a significant reduction in myelinated fibers, alongside elevated expression of tumor necrosis factor-alpha (TNF-α). Moreover, CIS induces glial cell activation, thereby promoting the upregulation of pro-inflammatory cytokine, including interleukin-1β and interleukin-6. In addition, MDA levels is raised, However, the level of SOD is reduced. CIS-triggered cytokine release activates nuclear factor kappa B (NF-κB), that promotes inflammation and oxidative stress, contributing to tissue damage and neurotoxicity [28-31]. This explained the presence of inflammatory cells in CIS group.

In the current work, a significant elevation ($P < 0.01$) of collagen fiber content in group II was observed, consistent with recent studies demonstrating that CIS- induces up-regulation of transforming growth factor beta (TGFβ), a key mediator of tissue fibrosis. CIS induces the upregulation of profibrotic proteins, including laminin and collagen. Also CIS-provoked oxidative stress activates NF-κB which sequentially induces fibrosis [32-36].

In this study toluidine blue- stained sections from group II displayed variable histological changes affecting myelin sheath and axon, in agreement with recent studies [37- 41].

Kassab& Elkaliny, (2017) [42] concluded that sciatic nerve exhibited axonopathy (irregular compressed axoplasm, shrunken, atrophied axon, and separation from myelin sheath) and myleinopathy (splitting, vacuolations and irregular thickening) as a result of CIS toxicity. The observed effects could potentially be mediated by apoptotic processes as cell volume shrinkage (compressed axons) and irregular outline of axoplasm are features of apoptosis.

Herein, the electron microscopic examination of CIS-group exhibited degenerative changes of myelin sheaths and axons. SCs exhibited a small nucleus with irregular outline, and these results agreed with some authors [14,43-45], were explained by [46-48] who stated that ROS and mitochondrial dysfunction are pivotal factors in CIPN pathogenesis. Peripheral nerves with their long axons are prone to ROS because of increased phospholipid content and relatively weak cellular antioxidant defenses. Also, the axoplasm contains abundant mitochondria and many researches suggest that axonal cytotoxicity plays a role in CIPN.

Chayaburakul et al. (2023) [49] explained the presence of focal splitting that separated the lamellae of myelin suggesting a pathological reversal of the myelination process. Notably, there was a pronounced infiltration of cytoplasm into the space between the adjacent cytoplasmic leaflets considerably exceeding that observed under normal physiological circumstances. CIS treatment injured SCs, ultimately causing the disintegration and separation of the myelin sheath. Under normal circumstances, the lamellae of the myelin sheath are firmly apposed due to the presence of transmembrane myelin basic proteins (MBP), that binds the inner surfaces of the membrane layers, helping to hold them together by interacting with their lipid components.

Liu et al. (2019) [50] also stated that CIS damage MBP resulting in gaps between the cytoplasmic leaflets of the myelin sheath, leading to the widening of Schmidt-Lanterman (SL) clefts or the splitting of myelin lamellae—hallmarks of demyelination.

Compared to the CIS group, H&E stained sections of CIS+Tau group showed markedly fewer vacuolations and less splitting of myelin sheaths and less inflammatory infiltrate. Also, a significant reduction ($P < 0.01$) of collagen fiber deposition in CIS+Tau group relative to CIS group were noticed. Toludine blue - stained sections of CIS+Tau group showed well compacted myelin sheaths. However, few nerve fibers displayed vacuolations and splitting of myelin. Moreover, EM showed mostly intact myelinated fibers with compact sheaths and stippled axoplasm. SCs exhibited normal nuclei, RER, and mitochondria. Some fibers showed myelin splitting, consistent with recent studies [51-56]. The EM observations align with the H&E and toluidine blue findings.

The significant histological improvement of the sciatic nerve may be attributed to Tau protective effects against oxidative stress, inflammation, and apoptosis. As reported by previous studies, Tau downregulates p53, caspase-3, Bax, TNF-α, and interleukin-6, while upregulating Bcl-2, SOD, and catalase gene expression. Its actions include ROS scavenging, inhibition of lipid peroxidation, Fe^{2+} chelation, osmoregulation, and enhancement of electron transport chain activity. [57-58]

In the present study Tau revealed a statically significant decrease ($P < 0.01$) of collagen fiber content in group

III relative to group II and this was explained by some researchers [59,60] who reported that Tau the expression of mRNA for NF-κB, consequently reducing the level of proinflammatory cytokines and fibrosis. Other researchers [61,62] demonstrated that Tau resulted in elevation of MBP expression and reduced SC apoptosis in the sciatic nerve.

In the present work, no histopathological changes were observed in group IV (Tau group). Statistical analysis of Masson trichome stained sections showed insignificant difference ($P > 0.01$) of collagen fiber deposition in group IV relative to group I. Toluidine blue-stained sections from group IV demonstrated preserved sciatic nerve architecture with intact myelinated fibers, clear axons, and minimal endoneurial connective tissue. Ultrastructurally, fibers displayed compact myelin, visible microtubules, and neurofilaments, with SC cytoplasm encasing axons findings consistent with Tau protective effect as noted by [63–65].

Conclusion

Histological and ultrastructural analyses revealed that taurine administration ameliorated the neurotoxic alterations induced by cisplatin, including nerve fiber disorganization, myelin degeneration and abnormal collagen deposition. Cisplatin + taurine group exhibited partial restoration of normal nerve architecture and a significant decrease in collagen fiber accumulation relative to the cisplatin-only group. These findings suggest that taurine may represent a promising neuroprotective agent to mitigate cisplatin-induced neurotoxicity in albino rats.

Limitations

Although the finding of this work are encouraging, certain aspects could be expanded in future work. It was limited to male albino rats, and functional and biochemical assessments were not included.

Recommendations

Future research should include both sexes and incorporate functional and biochemical assessments to correlate histopathological findings with functional outcomes and to further clarify the extent and mechanisms of neuroprotection. Additionally, exploring varied dosages and treatment durations is recommended.

References

[1] **Becker, G.; Atuati, S. F.; & Oliveira, S. M.** G Protein-Coupled Receptors and Ion Channels Involvement in Cisplatin-Induced Peripheral Neuropathy: A Review of Preclinical Studies. Cancers. (2024); 16(3):1-18.DOI:org/10.3390/ cancers1603058

[2] **Chovanec, M.; Abu Zaid, M.; Hanna, N.; El-Kouri, N.; Einhorn, L. H.; and Albany, C.** Long-term toxicity of CIS in germ-cell tumor survivors. Ann. Oncol. (2017); *28*(11), 2670-2679. DOI:10.1093/annonc/mdx360

[3] **Reynoso, J. P.; De Jesus Encarnacion, M.; Nurmukhametov, R.; Melchenko, D.; Efe, I. E.; Goncharov, E .et al.** Anatomical variations of the sciatic nerve exit from the pelvis and its relationship with the piriformis muscle: Acadaveric study. *Neurology international*. (2022); *14*(4):894-902. DOI:org/10.3390/neurolint14040072

[4] **Vallat, J. M., & Mathis, S.** Pathology explains various mechanisms of autoimmune inflammatory peripheral neuropathies. Brain Pathology. (2024);34(2):1-8. DOI: 10.1111/bpa.13184

[5] **Li, T.; Mizrahi, D.; Goldstein, D.; Kiernan, M. C.; & Park, S. B.** Chemotherapy and peripheral neuropathy. *Neurological Sciences.* (2021);*42*(10):4109-4121. DOI:org/10.1007/s10072-021-05576-6

[6] **Santulli, G.; Kansakar, U.; Varzideh, F.; Mone, P.; Jankauskas, S.S.; Lombardi, A.** Functional Role of Taurine in Aging and Cardiovascular Health: An Updated Overview. Nutrients. (2023); 15(19):1-18. DOI:org/10.3390/nu15194236

[7] **Li, Y.; Peng, Q.; Shang, J.; Dong, W.; Wu, S.; Guo, X .et al.** The role of taurine in male reproduction: Physiology, pathology and toxicol/ogy. Front. Endocrinol. (2023);14:1-16. DOI:org/10.3389/fendo.2023.1017886

[8] **Ibrahim, M.A.; Eraqi, M.M.; Alfaiz, F.A.** Therapeutic role of taurine as antioxidant in reducing hypertension risks in rats.Heliyon. (2020);6(1):1-9. DOI:org/10.1016/j.heliyon.2020.e03209

[9] **Gonullu, E.; Dagistan, G.; Erkin, Y.; Erdogan, M. A.; & Erbas, O.** Demonstration of the protective effect of propofol in rat model of CIS-induced neuropathy. Bratislavske Lekarske Listy. (2023);124 (1):64-69. DOI:org/10.4149/bll_2023_010

[10] **Azab, S. S.; Ismail, N. N.; Hosni, H. E. D.; & Abd El Fatah, M.** The defensive role of taurine against gonadotoxicity and testicular apoptosis effects induced by CIS in rats. *Journal of Infection and Chemotherapy.* (2020*);26*(1):51-57. DOI:org/10.1016/j.jiac.2019.07.004

[11] **Bancroft, J. D. and Lyton. C.** The hematoxyline and eosin and Connective and other mesenchymal tissues with their stains Techniques. Eds. Suvarna, S. K.; Layton, C. and Bancroft, J. D. 8th ed. Ch.10& 12. (2019); Pp. 126-138& 153-175. Churchill Livingstone of El Sevier, Philadelphia.
ISBN: 978-0-7020-6864-5

[12] **Hayat, M.A.** Principles and techniques of electron microscopy. 4th ed. (2000); pp. 96 – 123. Cambridge University Press, UK.
DOI:10.1006/anbo.2001.1367

[13] **Amarelo, A.; da Mota, M. C. C.; Amarelo, B. L. P.; Ferreira, M. C.; & Fernandes, C. S.** Effects of Physical Exercise on Chemotherapy-Induced Peripheral Neuropathy: A Systematic Review and Meta-Analysis. *Pain Management Nursing.* (2025)*;26(2):212-221.* DOI:org/10.1016/j.pmn.2024.12.011

[14] **Zaki, S. M.; Mohamed, E. A.; Motawie, A. G.; & Fattah, S. A.** N-acetylcysteine versus progesterone on the CIS-induced peripheral neurotoxicity. Folia morphologica. (2018);77(2):234-245. DOI: 10.5603/FM.a2017.0090

[15] **Gu, M.; Cheng, X.; Zhang, D.; Wu, W.; Cao, Y.; & He, J.** Chemokine platelet factor 4 accelerates peripheral nerve regeneration by regulating Schwann cell activation and axon elongation. *Neural Regeneration Research.* (2024)*;19*(1):190-195. DOI:org/10.4103/1673-5374.375346

[16] **Alsalem, M.; Ellaithy, A.; Bloukh, S.; Haddad, M.; & Saleh, T.** Targeting therapy-induced senescence as a novel strategy to combat chemotherapy-induced peripheral neuropathy. *Supportive Care in Cancer.* (2024); *32*(1):85,1-7. DOI:org/10.1007/s00520-023-08287-0

[17] **Jangra, A.; Gola, P.; Singh, J.; Gond, P.; Ghosh, S.; Rachamalla, M. et al.** Emergence of taurine as a therapeutic agent for neurological disorders. *Neural Regeneration Research.* (2024)*; 19*(1): 62-68. *DOI:* 10.4103/1673-5374.374139

[18] **Onk, D.; Mammadov, R.; SuleyMan, B.; Cimen, F. K.; Cankaya, M.; Gul, V.; .et al.** The effect of thiamine and its metabolites on peripheral neuropathic pain induced by CIS in rats. Experimental animals. (2018); 67(2): 259-269. DOI:org/10.1538/expanim.17-0090

[19] **Abdelsameea, A. A.; & Kabil, S. L.** Mitigation of CIS-induced peripheral neuropathy by canagliflozin in rats. *Naunyn-Schmiedeberg's Archives of Pharmacology*. (2018); *391*: 945-952. DOI:org/10.1007/s00210-018-1521-5

[20] **Abdelrahman, A.; Abd Elhaliem, N.; Elnady, H.; Lotfy, A.; & Moghazy, H.** A comparative study between the effect of nerve growth factor and all-trans retinoic acid versus their combined use on taxol induced peripheral neuropathy in adult male albino rat. *Egyptian Journal of Histology*. (2019); *42*(2): 408-424. DOI: 21608/ejh.2019.7080.1063

[21] **Bilir-Yildiz, B.; Sunay, F. B.; Yilmaz, H. F.; & Bozkurt-Girit, O.** Low-intensity low-frequency pulsed ultrasound ameliorates sciatic nerve dysfunction in a rat model of CIS-induced peripheral neuropathy. Scientific Reports. (2022); 12(1), 8125:1-12. DOI.org/10.1038/s41598-022-11978-z

[22] **Khodir, S. A.; Imbaby, S.; Amer, M. S. A. A.; Atwa, M. M.; Ashour, F. A.; & Elbaz, A. A.** Effect of mesenchymal stem cells and melatonin on experimentally induced peripheral nerve injury in rats. *Biomedicine & Pharmacotherapy*. (2024); *177*:1-9. DOI:org/10.1016/j.biopha.2024.117015

[23] **Sharawy, N.; Rashed, L.; & Youakim, M. F.** Evaluation of multi-neuroprotective effects of erythropoietin using CIS induced peripheral neurotoxicity model. *Experimental and toxicologic pathology : official journal of the Gesellschaft fur Toxikologische Pathologie*. (2015); *67*(4):315–322. DOI:org/10.1016/j.etp.2015.02.003

[24] **Khademi, E.; Mahabadi, V. P.; Ahmadvand, H.; Akbari, E.; & Khalatbary, A. R.** Anti-inflammatory and anti-apoptotic effects of hyperbaric oxygen preconditioning in a rat model of CIS-induced peripheral neuropathy. Iranian Journal of Basic Medical Sciences. (2020); 23(3): 321-328. DOI:org/10.22038/IJBMS.2019.40095.9504

[25] **Mahmoud, H. A.; El Horany, H. E.; Aboalsoud, M.; Abd-Ellatif, R. N.; El Sheikh, A. A.; & Aboalsoud, A.** Targeting oxidative stress, autophagy, and apoptosis by quercetin to ameliorate CIS-induced peripheral neuropathy in rats. *Journal of Microscopy and Ultrastructure.)* (2023); *11*(2): 107-114. DOI: 10.4103/jmau.jmau_78_22

[26] **Ali, M. M.; & Aziz, T. A.** Toxic effect of platinum compounds: molecular mechanisms of toxicity. *Al-Rafidain Journal of Medical Sciences (ISSN 2789-3219).* (2021); *1*:81-88. DOI:org/10.54133/ajms.v1i.32

[27] **Fumagalli, G.; Monza, L.; Cavaletti, G.; Rigolio, R.; Meregalli, C.** Neuroinflammatory Process Involved in Different Preclinical Models of Chemotherapy-Induced Peripheral Neuropathy. Front. Immunol. (2021); 11:1-24. DOI:org/10.3389/fimmu.2020.626687

[28] **Li, C.; Deng, T.; Shang, Z.; Wang, D.; & Xiao, Y.** Blocking TRPA1 and TNF-α signal improves bortezomib-induced neuropathic pain. *Cellular Physiology and Biochemistry*. (2018); *51*(5): 2098-2110. DOI:org/10.1159/000495828

[29] **Saadati, H.; Noroozzadeh, S.; Esmaeili, H.; Amirshahrokhi, K.; Shadman, J.; & Niapour, A.** The neuroprotective effect of mesna on CIS-induced neurotoxicity: behavioral, electrophysiological, and molecular studies. *Neurotoxicity Research.* (2021); *39*(3):826-840. DOI:org/10.1007/s12640-020-00315-9

[30] **Alotaibi, M.; Al-Aqil, F.; Alqahtani, F.; Alanazi, M.; Nadeem, A.; Ahmad, S. F.et al.** Alleviation of cisplatin-induced neuropathic pain, neuronal apoptosis, and systemic inflammation in mice by rapamycin. *Frontiers in Aging Neuroscience*. (2022); *14*:1-12. DOI:org/10.3389/fnagi.2022.891593

[31] **Abadi, A. J.; Mirzaei, S.; Mahabady, M. K.; Hashemi, F.; Zabolian, A.; Hashemi, F.et al.** Curcumin and its derivatives in cancer therapy: Potentiating antitumor activity of CIS and reducing side effects. *Phytotherapy Research*. (2022); *36*(1):189-213. DOI:org/10.1002/ptr.7305

[32] **Wu, Y.; Barrere, V.; Han, A.; Andre, M. P.; Orozco, E.; Cheng, X.et al.** Quantitative evaluation of rat sciatic nerve degeneration using high-frequency ultrasound. *Scientific reports.* (2023); *13*(1):1-17. DOI:org/10.1038/s41598-023-47264-9

[33] **Yildirim, C.; Yamaner, H.; Örkmez, M.; Cangİ, S.; Bozdayi, M. A.; Tasdemir, D. et al.** Sinapic Acid Ameliorates Cisplatin-Induced Peripheral Neuropathy: An In Vivo and In Vitro Study. *Firat Universitesi Sağlik Bilimleri Tip Dergisi*. (2023);*37*(1):66-79. DOI:org/10.1007/s12012-022-09773-3

[34] **Türedi, S.; Yuluğ, E.; Alver, A.; Bodur, A.; & İnce, İ.** A morphological and biochemical

evaluation of the effects of quercetin on experimental sciatic nerve damage in rats. *Experimental and therapeutic medicine*. (2018); *15*(4): 3215-3224. DOI:org/10.3892/etm.2018.5824

[35] **Abd_elmonem, S. N.** The Possible Protective Role of Melatonin and Exosomes Derived from Mesenchymal Stem Cells on CIS Induced Testicular Injury in Adult Male Albino Rats: Histological and Immunohistochemical Study. *Egyptian Journal of Histology*. (2024); *47*(3):978-990. DOI:org/10.21608/ejh.2023.214373.1902

[36] **Sewelam, A. S.; Amin, M. A.; Abdelmohsen, S. R.; Mohammed, O. A.; Hashish, A. A.; Alfaifi, J.et al.** Tempol maintained the cellular integrity of the cerebellar cortex by preserving neuron survival, autophagy, glial cells, and synapses after CIS exposure. *Translational Research in Anatomy*. (2024); *35*:1-9. DOI:org/10.1016/j.tria.2024.100298

[37] **Donertas, B.; Cengelli Unel, C.; Aydin, S.; Ulupinar, E.; Ozatik, O.; Kaygisiz, B.et al.** Agmatine cotreatment attenuates allodynia and structural abnormalities in CIS induced neuropathy in rats. Fundamental & clinical pharmacology. (2018);32(3):288-296. DOI:org/10.5152/balkanmedj.2016.161110

[38] **Ünel, Ç. Ç.; Ayaz, B.; Aydin, Ş.; Ulupinar, E.; Özatik, O.; Kaygisiz, B.et al.** Protective effects of anandamide against CIS-induced peripheral neuropathy inrats. Turkish Journal of Medical Sciences. (2021); 51(6): 3098-3107. DOI:org/10.3906/sag-2101-224

[39] **Ismail, D. I.; & Farag, E. A.** A histological study on platelet poor plasma versus platelet rich plasma in amelioration of induced diabetic neuropathy in rats and the potential role of telocyte-like cells. *Egyptian Journal of Histology*. (2021); *44*(1):8-30. DOI:org/10.21608/ejh.2020.27619.1274

[40] **Zglejc-Waszak,K.; Mukherjee, K.; Korytko, A.; Lewczuk, B.; Pomianowski, A.; Wojtkiewicz, J.et al.** Novel insights into the nervous system affected by prolonged hyperglycemia. Journal of Molecular Medicine. (2023);101(8):1015-1028. DOI: org/10.1007/s00109-023-02347-y

[41] **Türedi, S.; Çelik, H.; Dağlı, Ş. N.; Taşkın, S.; Şeker, U.; & Deniz, M.** An Examination of the Effects of Propolis and Quercetin in a Rat Model of Streptozotocin-Induced Diabetic Peripheral Neuropathy. Current Issues in Molecular Biology. (2024); 46(3): 1955-1974. DOI:org/10.3390/cimb46030128

[42] **Kassab, A. A.; & Elkaliny, H. H.** The possible role of propolis in ameliorating paclitaxel-induced peripheral neuropathy in sciatic nerve of adult male albino rats. *Egyptian Journal of histology*. (2017); *40*(2): 141-155. DOI:org/10.21608/EJH.2017.4073

[43] **Fekry, E., Refaat, G. N., & Hosny, S. A.** Ameliorative Potential of Carvedilol Versus Platelet-Rich Plasma Against Paclitaxel-Induced Femoral Neuropathy in Wistar Rats: A Light and Electron Microscopic Study. *Microscopy and Microanalysis*. (2025); 31(1)**:**1-17. DOI:org/10.1093/mam/ozaf002

[44] **Chiang, A. C.; Seua, A. V.; Singhmar, P.; Arroyo, L. D.; Mahalingam, R.; Hu, J. et al.** Bexarotene normalizes chemotherapy-induced myelin decompaction and reverses cognitive and sensorimotor deficits in mice. *Acta Neuropathologica Communications*. (2020); *8*(1):1-15. DOI: 10.1186/s40478-020-01061-x

[45] **Wahdan, S. A.; Elsherbiny, D. A.; Azab, S. S.; & El Demerdash, E.** Piceatannol ameliorates behavioural, biochemical and histological aspects in CIS induced peripheral neuropathy in rats. Basic & Clinical Pharmacology & Toxicology. (2021); 129(6):486-495. DOI:org/10.1111/bcpt.13643

[46] **Lazić, A.; Popović, J.; Paunesku, T.; Woloschak, G. E.; & Stevanović, M.** Insights into platinum-induced peripheral neuropathy–current perspective. *Neural Regeneration Research*. (2020); *15*(9):1623-1630. DOI:org/10.4103/1673-5374.276321

[47] **Seto, Y.; Niwa, K.; Okazaki, F.; & To, H.** Time dependent CIS dosing differences on hypoalgesia focusing on oxidative stress. *European Journal*

of Pharmacology. (2023); *942*: 1-51. DOI:org/10.1016/j.ejphar.2023.175519

[48] **Wang, X.; Yang, W.; Wang, L.; Zheng, L.; & Choi, W. S.** Platinum-based chemotherapy induces demyelination of Schwann cells in oral squamous cell carcinoma treatment. *Toxicology and Applied Pharmacology*. (2023); *481*: 1-8. DOI:org/10.1016/j.taap.2023.116751

[49] **Chayaburakul, K.; Ong, W. Y.; Herr, D. R.; Kobutree, P.; & Chantra, K.** Differences in the ultrastructure of neurons in the spinal ganglion and dorsal rootlet between rats treated with CIS only versus co-administration with a sphingosine 1-phosphate receptor 2 agonist in attenuating neuropathy and allodynia. *Journal of the Peripheral Nervous System.* (2023)*; 28*(3):476-489. DOI:org/10.1111/jns.12582

[50] **Liu, B.; Xin, W.; Tan, J. R.; Zhu, R. P.; Li, T.; Wang, D. et al.** Myelin sheath structure and regeneration in peripheral nerve injury repair. *Proceedings of the National Academy of Sciences.* (2019); *116*(44): 22347-22352. DOI:org/10.1073/pnas.1910292116

[51] **Kucu, A.; Ozyigit, F.; Akcer, S.; Tosun, M.; Kocak, F. E.; & Kocak, A.** Investigation of the effect of taurine on sciatic nerve ischemia-reperfusion injury in rats. *Basic Res J Med Clin Sci*. (2015); *4(8)*: 223-230.

[52] **Li, K.; Shi, X.; Luo, M.; Wu, P.; Zhang, M.; Zhang, C. et al.** Taurine protects against myelin damage of sciatic nerve in diabetic peripheral neuropathy rats by controlling apoptosis of schwann cells via NGF/Akt/GSK3β pathway. *Experimental cell research.* (2019);*383*(2):1-11. DOI:org/10.1016/j.yexcr.2019.111557

[53] **Zhang, M.; Shi, X.; Luo, M.; Lan, Q.; Ullah, H.; Zhang, C. et al.** Taurine ameliorates axonal damage in sciatic nerve of diabetic rats and high glucose exposed DRG neuron by PI3K/Akt/mTOR-dependent pathway. *Amino acids.* (2021);*53(3)*:395-406. DOI:org/10.1007/s00726-021-02957-1

[54] **Ai, A.; Saremi, J.; Ebrahimi-Barough, S.; Fereydouni, N.; Mahmoodi, T.; Sarikhani, P. et al.** Bridging potential of Taurine-loading PCL conduits transplanted with hEnSCs on resected sciatic nerves. *Regenerative Therapy*. (2022);*21(1)*:424-435. DOI:org/10.1016/j.reth.2022.09.004

[55] **Ehterami, A.; Rezaei Kolarijani, N.; Nazarnezhad, S.; Alizadeh, M.; Masoudi, A.; & Salehi, M.** Peripheral nerve regeneration by thiolated chitosan hydrogel containing taurine: in vitro and in vivo study. *Journal of Bioactive and Compatible Polymers*. (2022) ; *37*(2): 85-97. DOI:org/10.1177/08839115221085736

[56] **Wang, Y.; Gao, B.; Chen, X.; Shi, X.; Li, S.; Zhang, Q. et al.** Improvement of diabetes-induced spinal cord axon injury with taurine via nerve growth factor-dependent Akt/mTOR pathway. *Amino Acids. (2024)* ; *56*(1):1-13. DOI:org/10.1007/s00726-024-03392-8

[57] **Niu, X.; Zheng, S.; Liu, H.; & Li, S.** Protective effects of taurine against inflammation, apoptosis, and oxidative stress in brain injury. *Molecular medicine reports*. (2018);*18*(5): 4516-4522. DOI:org/10.3892/mmr.2018.9465

[58] **Abou El-khair, A. R.; Ghanem, N.; Soliman, M. M.; Aldhahrani, A.; Farag, M. R.; Abd El-Hack, M. E. et al.** Ameliorative impact of taurine on oxidative damage induced by Ipomoea carnea toxicity in wistar male rats through modulation of oxidative stress markers, apoptotic and Nrf2 pathway. *Journal of King Saud University-Science*. (2021);*33*(8): 1-10. DOI:org/10.1016/j.jksus.2021.101639

[59] **Younis, N. S.; Ghanim, A. M.; Elmorsy, M. A.; & Metwaly, H. A.** RETRACTED ARTICLE: Taurine ameliorates thioacetamide induced liver fibrosis in rats via modulation of toll like receptor 4/nuclear factor kappa B signaling pathway. *Scientific Reports.* (2021); *11*(1):1-17. DOI:org/10.1038/s41598-021-91666-6

[60] **Naderi, M.; Seyedabadi, M.; Amiri, F. T.; Mohammadi, E.; Akbari, S.; & Shaki, F.** Taurine protects against perfluorooctanoic acid-induced hepatotoxicity via inhibition of oxidative stress, inflammatory, and

apoptotic pathways. *Toxicology research*. (2023);*12*(1):124-132. DOI:org/10.1093/toxres/tfad005

[61] **Gu, Y.; Zhao, Y.; Qian, K.; & Sun, M.** Taurine attenuates hippocampal and corpus callosum damage, and enhances neurological recovery after closed head injury in rats. *Neuroscience.* (2015); *291*:331-340. DOI:org/10.1016/j.neuroscience.2014.09.073

[62] **Li, K.; Shi, X.; Luo, M.; Wu, P.; Zhang, M.; Zhang, C. et al.** Taurine protects against myelin damage of sciatic nerve in diabetic peripheral neuropathy rats by controlling apoptosis of schwann cells via NGF/Akt/GSK3β pathway. *Experimental cell research.* (2019); *383*(2):1-11. DOI:org/10.1016/j.yexcr.2019.111557

[63] **Sun, G.; Qu, S.; Wang, S.; Shao, Y.; & Sun, J.** Taurine attenuates acrylamide-induced axonal and myelinated damage through the Akt/GSK3β-dependentpathway. *International journal of immunopathology and pharmacology.* (2018); *32*:1-10**.**DOI:org/10.1177/2058738418805322

[64] **Khalil, R. M.; Abdo, W. S.; Saad, A.; & Khedr, E. G.** Muscle proteolytic system modulation through the effect of taurine on mice bearing muscular atrophy. *Molecular and cellular biochemistry*. (2018);*44*(1-2): 161-168. DOI:org/10.1007/s11010-017-3240-5

[65] **Lee, C. C.; Chen, W. T.; Chen, S. Y.; & Lee, T. M.** Taurine alleviates sympathetic innervation by inhibiting NLRP3 inflammasome in postinfarcted rats. *Journal of Cardiovascular Pharmacology*. (2021); *77*(6):745-755. DOI:org/10.1097/fjc.0000000000001005

To cite this article: Shereen M. Mostafa , Maysara A. Salem, Hamdy A. Mohamed, Enas Elgendy. Histological Study on the Effect of Taurine on Cisplatin Induced Sciatic Nerve Neuropathy in Adult Male Albino Rats. BMFJ XXX, DOI: 10.21608/bmfj.2025.397488.2494